Combining plot measurements and a calibrated RUSLE model to investigate recent changes in soil erosion in upland areas in Southern Italy

Combining plot measurements and a calibrated RUSLE model to investigate recent changes in soil erosion in upland areas in Southern Italy

P. Porto, M. Bacchi, G. Preiti, M. Romeo, M. Monti

Department of AGRARIA, University Mediterranea, Feo di Vito, 89122 Reggio Calabria, Italy

✉ Paolo Porto

paolo.porto@unirc.it

Abstract

Purpose In recent decades, soil erosion has been recognized as a serious environmental problem in many countries of the world and the impacts of climate change have focused attention on potential changes in erosion rates that could further increase such problem. These impacts are documented by a general decrease of annual precipitation and a corresponding increase in the number of heavy rainfall events, intensity and frequency that accelerate the loss of fertile soil material.

Materials and methods Direct observations of soil loss obtained during the period 2006-2016 on five experimental plots in Southern Italy were preliminarily presented and discussed. These measurements~~, using a calibrated~~ were used to calibrate the RUSLE model that, coupled with independent long-term measurements of rainfall erosivity, allowed calculation of soil erosion from 1954 to date.

Results and discussion The plot measurements showed annual values of soil erosion generally higher than the long-term estimates provided by the RUSLE (1954-2019) suggesting an increasing trend of soil erosion rates during the last 20-25 years. On the contrary, a decreasing trend of the annual rainfall measurements can be observed for the same period.

Conclusions The overall results demonstrated that models like the RUSLE can be considered a useful tool to individuate changes of erosion rates and to isolate the effect of climate change on soil loss. Also, the opposite trend obtained for the annual rainfall measurements suggests that these should not be used to explore the effects of climate change in Mediterranean areas but measurements of rainfall at shorter time intervals (≤ 30 minutes) are necessary.

Keywords Soil erosion • Experimental plots • RUSLE • Climate change • Southern Italy.

1 INTRODUCTION

In the last decades, the impact of climate change on human activities and world economy has attracted increasing interest from the scientific community. According to IPCC (2018), a general increase of temperature and a change in precipitation trends have been documented by many studies over the world (Dore 2005; Alexander 2016). Specific examples are provided in USA by Karl and Knight (1998) that, analysing secular trends of rainfall, established that a general increase in precipitation, reflected primarily in the heavy and extreme daily precipitation events, can be observed. Similar results, related to the intensity distribution of daily precipitation amounts, were observed by Osborne et al. (2000) in UK, Suppiah and Hennessy (1998) in Australia, and Mason et al. (1999) in South Africa. In central and western Europe, Moberg and Jones (2005) documented a significant increase of precipitation trends over the 20th century for both average precipitation intensity and moderately strong events. Recent studies carried out in southern Italy indicated a general increase in the number of heavy precipitation events, intensity and frequency since about 1950 (Capra et al. 2017).

These effects have important consequences for environmental risks such as floods, landslides, and land degradation. The latter includes both rates of soil erosion in upland cultivated areas and sediment delivered downstream. The effects of soil erosion in cultivated areas consist mainly of reducing soil productivity and food security (on-site effects) by loss of organic matter and crop yield depression that increases the risk of land abandonment (Kolouri and Giourga 2007; Romero-Díaz et al. 2017) and the decline of rural community (Bakker et al. 2005). The effects caused by the amount of sediment generated in the upland areas and delivered downstream (off-site effects) are ~~even more~~also dangerous as they can increase pollution of rivers (Boardman and Poesen 2006; Yi et al. 2008; Wen et al. 2017), reduce water resources in the reservoirs (Pimentel et al. 1995; De Araújo et al. 2006), and affect the stability of aquatic ecosystems (Palmer et al. 2009).

However, problems of land degradation are also affected by other drivers such as urban sprawl, changes in land use, land abandonment, and other social factors (Shao et al. 2021). For these reasons, in the absence of specific experimental sites able to produce field measurements, it is difficult to establish the precise causes of land degradation. In this context, documenting rates of soil erosion in ~~representative~~ specific experimental sites that are representative of contexts of similar characteristics can be an important tool to understand better the consequences of climate change on ~~larger areas~~larger areas and on long-term temporal scale.

Experimental plots, equipped specifically for monitoring rainfall, runoff and soil loss, proved to be an important means to obtain information on the impacts of soil properties, land use, crop management etc. on erosion rates ~~erosion rates~~ because external factors are under control (Loughran 1989). However, despite their utility, some difficulties to extrapolate the results for larger spatial scales or different time windows for which no direct measurements are available must be recognized (see Ev~~w~~ans 1995; Boardman 2006). In recent years, the attempt to compile an extensive database of short to medium-term erosion rates as measured on erosion plots in Europe and Mediterranean regions under natural rainfall was made by several authors (see Cerdan et al. 2010; Maetens et al. 2012). Even if this effort produced the largest (227 plot-measuring sites) database of plot runoff and soil loss data in Europe (Maetens et al. 2012), these measurements are frequently limited to the period of the experiments (normally, a few years) and it is difficult to extend their temporal trend in the absence of retrospective information. In other words, this large dataset is very useful to investigate the effects of land use, soil type and topography but insufficient data about climate precludes any statistical analysis aimed at identifying possible trends in soil erosion rates (see Cerdan et al. 2010). In such situations, the use of calibrated models, in which the climate component is taken into account, can be very useful.

In this respect, numerical models of different generations have been employed to predict soil loss in the absence of direct measurements during the last decades. These models can be based on empirical approaches, such as the Universal Soil Loss Equation (Wischmeier and Smith 1978) and its derived version (Renard et al. 1994), on simple correlation analyses between soil erosion and topography (Bagarello et al. 2011; 2018), or on more complex algorithms of calculation that interpret physical processes related to detachment and transport of soil particles (Nearing et al. 1989). However, even if their use proved to be very effective for a short-time scale, it is important to note that such models should be calibrated and validated to provide reliable results for larger time windows in which possible effects due to climate change can be expected. Results in this direction were obtained by several authors. Chaplot (2007) and Ficklin et al. (2009), for example, explored the performance of the SWAT model to predict long-term soil loss in cultivated areas of the USA. Pandey et al. (2017), in India, tested the hydrological component of the SWAT model in areas affected by climate change. Pruski and Nearing (2002a,b) provided long-term simulations of soil loss using WEPP coupled with historical rainfall datasets available in three different locations of the USA. Pal and Chakrabortty (2019) made a long-term application of the RUSLE model to evaluate the impact of climate change on soil erosion in sub-tropical monsoon areas in the West Bengal state of eastern India. Favis-Mortlock and Boardman (1995) used the EPIC model to evaluate changes on erosion rate in the UK. However, it must be recognized that most of these contributions, even if USLE derived, are based on simulation exercises in which the rainfall erosivity is not calculated using the basic approach proposed by Wischmeier and Smith (1978) that requires the knowledge of rainfall energy at event scale, but it is derived from indirect relationships with daily or monthly rainfall, using simplified approaches like Arnoldus index (Pal and Chakrabortty 2019) or applying more sophisticated climate generators like CLIGEN (Pruski and Nearing 2002a,b). The importance of direct observations of rainfall erosivity was emphasized by Wischmeier and Smith (1978) that suggested a period of at least 22 years of measurements for calculating the R-factor (Renard et al. 1997). However, as pointed out by Verstraeten et al. (2006), this period of 22 years is recommended because very few detailed rainfall data records exist for a longer time period in areas outside the USA where the USLE was developed. Verstraeten et al. (2006), provided an example of long-term dataset of rainfall erosivity analysing a record of 10-min rainfall (105 years) in Belgium. These authors established that average 10-year erosion rates calculated with the RUSLE have increased by 24–34% from the first decade (1903–1912) to the last one (1993–2002) of the study period, as a consequence of changing rain erosivity through time and encouraged the use of long-term records of short time-interval rainfall in simulation exercises.

Recent studies carried out at a plot scale in Southern Italy documented high rates of soil erosion both on cultivated lands (Bagarello et al. 2010) and in areas subject to afforestation that support discontinuous forest cover (Khodadadi et al. 2020). In these areas, several attempts to calibrate and validate numerical models like RUSLE (Di Stefano et al. 1999), MUSLE (Cinnirella et al. 1998), USLE-M (Bagarello et al. 2018), and SEDD (Porto and Callegari 2021) have been successful in their ability to reproduce soil erosion rates or sediment yield both at plot and at catchment scale for short time windows. However, the absence of long-term measurements and the general difficulty of obtaining equivalent records of model input parameters like rainfall erosivity or crop factors precluded specific studies aimed at investigating long-term soil erosion rates in Italy. A few exceptions are related to the combined use of radiotracers ^{137}Cs and ^{210}Pb$_{ex}$ that in view of their ability to obtain retrospective information on soil erosion for different time windows provided important results in this direction (see Porto et al. 2016; 2018).

In this contribution, direct observations of soil erosion obtained in 5 experimental plots during 11 years of investigation were combined with a long-term record of rainfall erosivity to reconstruct a trend of soil loss in a typical upland area of Southern Italy. More specifically, the measurements of soil loss served to calibrate the RUSLE model for cultivated soils supporting typical Mediterranean crops and the rainfall erosivity data were used to derive estimates of erosion rates during the last 6-7 decades. This experiment provided evidence of a change of erosion rates during the last 2-3 decades emphasizing the effect of climate change on soil erosion in cultivated lands in Mediterranean areas.

2 MATERIAL AND METHODS

The study area (38°16’ N, 15°49’ E) is located in Calabria, Southern Italy at an elevation of 585 m a.s.l. (Fig. 1). The climate is typically Mediterranean, characterized by a rainy season extending from October to March and a dry summer during which occasional thunderstorms may occur. The annual precipitation (*Pa*), measured at the rainfall station of Santa Cristina d’Aspromonte, is approximately 1470 mm (Arpacal datasets 1939-2019). Mean annual temperatures range from

14 °C to 15 °C, based on local reports (Arpacal datasets 1988-2020). The land use is characterized by cultivated soils where traditional arable and vegetable crops are grown. In 2005, the Department of Agraria of the University 'Mediterranea' of Reggio Calabria established five (5m x 25m) experimental plots (Fig. 1) to explore the effect of different cropping systems on runoff and soil loss (Preiti et al. 2017).

Fig. 1 – The study area and the experimental plots

The plots were built on a 10% slope and support Typic Hapludands soils characterised by a silty loam texture (20% sand, 76% silt, and 4% clay). The plots were established, with minimum soil disturbance, over an area subject to traditional cultivation in order to make the measurements representative for the local area. In this respect, plot 1 has been maintained bare since the beginning of the experiment, by up and down slope tillage operations according to Wischmeier and Smith (1978). Three plots (plot 2, 3, and 4) have supported different crops typical of the area that include rye, lupin, wheat, oat, cauliflower, sorghum, potatoes, tall fescue, horseradish, aubergines, trifolium. These were cultivated using similar management systems but with different inter-annual rotations. Plot 5 was covered mainly by natural vegetation, tall fescue and lupin and was subjected to minimal tillage and crop operations during the last six years of measurements. Also, crop residues were left on soil surface after each tillage operation. This choice was made to explore the effect of conservative techniques on soil loss (for soil and crop management details see Preiti et al. 2017).

Runoff and soil loss were measured for each plot, at event scale, for the period 2006-2016. More specifically, the runoff and soil loss were collected by gutters installed along the lower ends of each plot and diverted into a sized tank located at the base of the plot (see Fig. 1). Sampling of water and sediment stored in the tanks was undertaken two-three days after the end of each rainfall event. The sediment deposited on the bottom of the tank was collected and transported to the laboratory of the Department of Agraria where it was oven dried at 60 °C and weighed to determine its mass. The measurements of soil loss used in this experiment are related to 135 events that have occurred during the period from January 2006 to December 2016.

3 RESULTS

3.1 The measured values of soil loss obtained for the study period

The empirical frequency of the total annual soil losses obtained for the period 2006-2016 is illustrated in Fig. 2 for each experimental plot.

Fig. 2 – Values of soil loss obtained from each plot for the study period 2006-2016. The graph in (a) shows the frequency distribution of the annual values. The box plot in (b) indicates the data distribution~~Total annual (a) and mean (b) soil losses obtained from each plot for the study period 2006-2016. The vertical bars in (b) indicate the standard error for each plot~~

In Fig. 2, ~~summary~~ data distribution ~~for the mean soil loss~~ from each plot during the study period ~~are~~ is also reported. These results point out both the inter-annual variability of soil loss that reflects changes in erosivity during the study period and the inter-plot variability related to the impact of different cropping practices on soil loss.

It is clear from Fig. 2 that the annual values of soil loss obtained from plot 1, in which vegetation cover was absent for most of the study period, are greater than those from the other plots. This result is expected because it emphasizes the importance of vegetation cover in the other plots that must be seen as a key factor in soil erosion studies. The mean value of soil loss related to plot 1 accounts for ca. 69.0 t ha^{-1} yr^{-1} (SE = 13.5 t ha^{-1} yr^{-1}). Even if this value is in line with the results obtained in areas where similar experiments were conducted (see Bagarello et al. 2018), it cannot be considered representative of a long-term pattern of land use in the area because it reflects the bare conditions maintained in this plot for the duration of the experiment (11 years). The mean values of soil loss obtained from the other plots range from 14.4 t ha^{-1} yr^{-1} (SE = 7.0 t ha^{-1} yr^{-1}), obtained from plot 5, to 39.2 t ha^{-1} yr^{-1} (SE = 11.7 t ha^{-1} yr^{-1}) obtained from plot 3. These values, reported in Table 1, reflect the different crop rotations adopted in the plots and indicate the crop system related to plot 5, which was subjected to minimal tillage and crop operations, as the most conservative in the area.

3.2 The calibration of the RUSLE model using the experimental data

As reported above, the study period extended for 11 years and these measurements, considering the number of events (135) occurred during the experiment, offer an important tool to calibrate soil erosion models in order to obtain soil loss estimates for a longer period. The available datasets and the size of the plots suggested the use of the RUSLE model to make such attempt. This calibration exercise was based on the following version of the USLE as originally proposed by Wischmeier and Smith (1978):

$$A_i = R_i\, K\, LS\, C_i\, P \qquad (1)$$

in which, the soil loss, A_i, is expressed in t ha^{-1} yr^{-1}; the rainfall erosivity factor, R_i, is expressed in MJ mm ha^{-1} h^{-1} yr^{-1}; the soil erodibility factor, K, is expressed in t ha h ha^{-1} MJ^{-1} mm^{-1}; LS represents the topographic factor (dimensionless); C_i represents the cover and management factor (dimensionless), and P indicates the support practice factor (dimensionless).

In this contribution, the Eq. (1) was calibrated at annual scale and the subscript i represents the i-th year for which soil loss observations are available. It is worth noticing that, because of the absence of support practices, the P-factor was set equal to 1.

The model calibration was carried out in three steps: the first step is related to the calculation of the factors R_i and LS that required rainfall and topographic measurements, respectively; the second step aimed at calculating the soil erodibility factor K; the third step allowed the calculation of the C_i values for each plot~~the calculation of the *C*-factor for each plot~~. These factors were determined as follows.

Formatted: Font: Italic

Formatted: Font: Italic, Subscript

Formatted: Subscript

3.2.1 The rainfall erosivity factor and the topographic factor

The rainfall erosivity factor R, as defined by Wischmeier and Smith (1978), represents the mean annual value of ~~the rainfall erosion index, *EIR*~~$_i$, calculated by summing the values of the rainfall erosion index, EI~~, values~~ obtained for each erosive event. The calculation of EI (MJ mm ha^{-1} h^{-1}) for each individual storm required a continuous record of rainfall intensity and it was determined by the product of total storm energy E (MJ ha^{-1}) and maximum 30-min intensity i_{30} (mm h^{-1}):

Formatted: Font: Italic

Formatted: Subscript

$$EI = E\, i_{30} = \left(\sum_{j=1}^{m} e_j \, \Delta V_j \right) i_{30} \tag{2}$$

with e_j indicating the rainfall energy per unit depth of rainfall per unit area, and ΔV_j the rainfall depth for the j-th interval of the storm hyetograph which is divided into m parts with essentially constant intensity. The equations proposed by Foster et al. (1981) were used to calculate the rainfall energy e_j:

$$e_j = 0.119 + 0.0873 \log_{10}(i_j) \qquad \text{if } i_j \le 76\ mm h^{-1} \tag{3a}$$

$$e_j = 0.283 \qquad \text{if } i_j > 76\ mm h^{-1} \tag{3b}$$

where i_j (mm h^{-1}) is the rainfall intensity calculated as follows

$$i_j = \frac{\Delta V_j}{\Delta t_j} \quad (4)$$

in which Δt_j indicates the interval duration over which intensity is assumed to be constant (Porto 2016). The rainfall record used in this contribution was obtained from the local station of Santa Cristina d'Aspromonte (Arpacal datasets), for which data with a temporal resolution Δt = 5 min were available. The mean value of the rainfall erosivity factor *R* calculated from this station for the study period 2006-2016 is reported in Table 1.

The topographic factor, *LS* (dimensionless), was calculated using the equation proposed by McCool et al. (1987), (Renard et al. 1994):

$$LS = (\lambda_i/22.13)^{m_i} \times (16.8 \operatorname{Sin} \alpha_i - 0.5) \quad (5)$$

considering that, for the study plots, *tan* $\alpha_i > 0.09$, with α_i representing the slope angle.

In eq. (5), λ_i indicates the slope length of the plot and the exponent m_i is given by the equation proposed by McCool et al. (1989):

$$m_i = \frac{f_i}{1 + f_i} \quad (6)$$

where f_i represents the ratio of rill to interrill erosion and can be expressed by the following formula:

$$\mathrm{f_i} = \frac{\sin \alpha_\mathrm{i}}{0.0896\left(3 \sin^{0.8} \alpha_\mathrm{i} + 0.56\right)} \quad (7)$$

The value of *LS*, that is assumed constant in each plot for the study period, is reported in Table 1.

Table 1 – The values of the RUSLE parameters obtained for each plot for the study period (2006-2016). In the last two columns are also reported the mean values of soil loss (A_i) measured during the study period (2006-2016) and those related to the long-term simulation (1954-2019).

Formatted: Justified

3.2.2 The soil erodibility factor *K*

The soil erodibility factor *K*, as defined by Wischmeier and Smith (1978), represents the mean annual value of the relative inherent resistance of a soil to the detachment, entrainment and transport actions operated by rainfall and runoff. The *K*-factor can be determined according to certain soil characteristics that include texture, presence of organic matter, permeability. In this respect, Wischmeier et al. (1971) provided a nomograph, supported by an explicit equation, to determine the value of *K* based on the above variables. However, if soil loss measurements are available at a plot scale, a direct evaluation of *K* is possible. The method is based on a simple regression analysis between soil loss measurements and rainfall erosivity, as proposed by Wischmeier and Mannering (1969), using the USLE unit plot (22.1 m long with a uniform 9% slope, continuously maintained in a clean-tilled fallow condition with upslope and downslope tillage).

Fig. 3 – Calculation of the soil erodibility factor *K*

In this contribution, we used the annual measurements of soil loss from the bare plot to obtain a representative value of *K* for the soils under investigation. Considering that our bare plot has a length of 25 m and a slope of 10%, an adjustment was necessary according to eq. (1). In other words, plotting the annual values of soil loss obtained from the bare plot against the corresponding values of the product R_iLS, assuming that the *C*-factor and the *P*-factor are equal to 1, it was possible to use the slope of the computed least-squares regression line, passing through the origin, to determine *K*. The method is illustrated in Fig. 3 in which the line of equation *y*=~~*mx*~~ *bx* is superimposed on the experimental pairs. The slope ~~*m*~~*b*, that represents the value of *K*, resulted equal to 0.011 (t ha h ha^{-1} MJ^{-1} mm^{-1}) and this value was assumed to be representative for our plots.

3.2.3 The cover and management factor C

The availability of soil loss measurements, together with the calculation of R_i and *LS*, and the direct determination of *K* from the bare plot, made it possible to derive the values of ~~the cover and management factor~~ C_i for the plots 2, 3, 4, and 5 in which different combinations of cropping systems were adopted during the 11 years of investigation. Again, this calibration exercise was carried out using the annual data of soil loss A_i and the following equation (Cinnirella et al. 1998):

$$C_i = \frac{A_i}{R_i\ K\ LS} \tag{8}$$

in which, for each plot, C_i is the value representing the crop factor for the year *i*.

Formatted: Subscript

Formatted: Subscript

The results of eq. (8) are summarized in Fig. 4~~,~~ where ~~the~~ the frequency distribution of C_i values~~single values of C_i and their frequency distribution are~~ is reported for each plot.

A visual inspection of Fig. 4 suggests that the values of C_i show evidence of an interannual variability for each single plot and document a significant difference from plot to plot. These findings are expected because the values of C_i depend both on the cropping system adopted in each period and on the value of the rainfall erosivity factor calculated for that corresponding period. For this reason, it is difficult to choose a representative value of C for each plot as it assumes the meaning of a random variable.

It can be seen from Fig. 4 that each frequency distribution follows, approximately, a log-normal distribution (see dotted line superimposed in each graph) that suggests the presence of a random component. Based on these findings, we decided to calculate the value of Cm that produced the perfect agreement between measured and calculated soil loss for the study period and we assumed this value as the C~~-factor~~$_i$ value representative for each plot. The four values of Cm resulting from this calculation are also reported in Table 1.

Fig. 4 – The frequency distribution of ~~the~~ C~~-factor~~$_i$ for each plot. The dashed line represents a log-normal theoretical distribution

The cropping systems supported by the plots 2, 3, 4, and 5 are typical of the cultivation techniques practiced in the upland areas of Southern Italy since the early 50s. For these reasons, the values of Cm reported in Table 1 can be considered representative of a long-term period in these areas. The same considerations can be extended to the mean value of the K-factor that can be assumed characteristic for this type of soil. Following this logic, in the absence of support practices and assuming a constant value of LS, only the rainfall erosivity factor R_i would affect the temporal variability of soil loss and it can be used to reconstruct the trend of soil erosion rates since the early 50s if a long-term dataset of R_i~~R~~ is available.

The annual values of R_i were obtained using the rainfall data available at the local station of Santa Cristina d'Aspromonte since 1954. These measurements were produced by the Italian Hydrographic Service at different temporal resolutions: the data for the period 1990-2019 are available at a time interval Δt = 5 min, with some short breakdown (Arpacal Datasets); the data for the period 1954-1989 were provided in a graphical form that required manual digitization to allow calculation of R_i at a temporal resolution of 30 minutes (see Wischmeier and Smith 1978). In order to get the values of precipitation amount and intensity consistent with those derived from the second dataset, the 5-minute data available for the period 1990-2019 were aggregated at a 30-minute temporal scale and the corresponding values of R_i were calculated accordingly (Porto 2016).

Formatted: Font: Italic

Formatted: Font: Italic, Subscript

Formatted: Font: Italic, Subscript

Formatted: Font: Italic, Subscript

Calculation of R_i for the missing years (1954-2005 and 2017-2019) and the availability of a calibrated RUSLE model for the shorter study period (2006-2016) allowed the reconstruction of soil erosion rates for the period 1954-2019. This calculation was made by hypothesizing 4 scenarios, one for each plot, in which only the C~~-factor,~~$_i$ was considered different from plot to plot and assumed equal to the C_m values listed in Table 1. The results of these predictions are illustrated in Fig. 5, where the values of soil loss A_i (t ha^{-1}) are reported in graphical form for each year. It is worth noticing that the predicted values of A_i (t ha^{-1}) are related to the two periods 1954-2005 and 2017-2019 for which soil erosion measurements are absent. On the contrary, the values of A_i (t ha^{-1}) for the study period 2006-2016 are those measured by the experimental device~~ and incorporated into the long-term record of Fig. 5~~. The mean values of soil loss for the period 1954-2019, that include measured and estimated data, are reported in Table 1.

Fig. 5 – The annual soil loss reconstructed for each plot for the period 1954-2019. Grey bars indicate the estimated values while white bars report the measured values obtained for the study period

~~In order to confirm this hypothesis~~The datasets illustrated in Fig. 5 were processed by~~,~~ a standard trend analysis test ~~was~~ performed using the software TREND (2012). More specifically, the Cumulative Deviation Test and the Student's *t* Test were carried out for each scenario in order to see if the means in two parts of each record are different (for an unknown time of change). The overall results suggested, at a level of probability $P<0.05$, that, for each scenario, the mean for the period 1954-1995 is significantly lower than the mean related to the period 1995-2019 and ~~confirmed the above hypothesis~~indicated that soil loss has not been stationary over the past 66 years.

4 DISCUSSION

The histograms illustrated in Fig. 5 and the mean values of soil loss reported in Table 1 provide important information on the magnitude of soil erosion since 1954 and offer a basis to understand the longer-term variability of soil loss in this area. The mean values of soil loss (plot measurements) related to the study period 2006-2016 are systematically higher than the corresponding long-term estimates for the period 1954-2019 (see Table 1). Also, a first visual inspection of the four graphs in Fig. 5 together with the linear trend overlaid on each figure suggests that soil loss shows an increasing trend for the period covered by this study. ~~In order to confirm this hypothesis, a standard trend analysis test was performed using the software TREND (2012). More specifically, the Cumulative Deviation Test and the Student's *t* Test were carried out for each scenario in order to see if the means in two parts of each record are different (for an unknown time of change). The overall results suggested, at a level of probability P≤0.05, that, for each scenario, the mean for the period 1954-1995 is significantly lower than the mean related to the period 1995-2019 and confirmed the above hypothesis that soil loss has~~

Formatted: Font: Italic, Subscript

~~not been stationary over the past 66 years.~~ These results are consistent with the work of Verstraeten et al. (2006) that observed an increase of an average 10-year erosion rate calculated in Belgium with the RUSLE as a consequence of changing rainfall erosivity through time. In fact, these changes reflect the temporal trend of R_i reported in Fig. 6 and are a consequence of a general increase in the magnitude of the rainfall erosivity during this period. In this respect, Verstraeten et al. (2006) observed a significant increase of the R-factor in central Belgium for the period 1991–2002 compared to the period 1898–1990, and suggested that care must be taken when a single, invariant, value of R is adopted for simulating long-term scenarios of soil loss. In our experimental site, a statistical interpretation of R_i, based on the Mann-Kendall test and the linear trend test (Hirsch et al. 1992), established that an increasing trend for this variable can also be recognized at a level of probability $P \leq 0.10$ and this provides a further confirm of the above hypothesis. Similar results were obtained in a simulation study conducted by Pruski and Nearing (2002a) that explored the effects on soil erosion in three locations of the USA by combining changes of rainfall intensity and number of rainy days over time. In that case, the simulation scenarios obtained with CLIGEN, even if in line with our findings, were never confirmed by empirical evidence.

Fig. 6 – The annual values (R_i) of the ~~R~~ rainfall erosivity factor obtained for the period 1954-2019 (a) and the annual values of rainfall measured in the same period (b)

However, the results summarized in Fig. 6 pose another important question whether an accurate estimate of R_i requires a proper relationship between rain intensity and rain kinetic energy or whether a simple correlation analysis between rainfall erosivity and rainfall amount can be adopted. In order to answer the above question, the annual rainfall *Pa* for the corresponding period (1954-2019) is also reported in Fig. ~~7~~6. Surprisingly, the histograms of Fig. ~~7~~ 6 show a decreasing trend of *Pa* in this area and a Cumulative Deviation Test suggested that this hypothesis cannot be rejected at a level of probability $P \leq 0.1$.

~~**Fig. 7** – The annual values of rainfall obtained for the period 1954-2019~~

These findings are really important because they suggest that a) the two variables (R_i and *Pa*) do not necessarily show the same temporal trends, and b) the *R*-factor cannot be predicted indirectly using rainfall data at annual scale but it is necessary to use the proper time intervals (5 min $\leq \Delta t \leq$ 30 min) (Buffoni et al. 1999; Brunetti et al. 2001, 2002, 2004; Porto 2016). In other words, the above results indicate that the use of simplified models like those provided by Fournier (1960) or Arnoldus (1980) that are based on monthly and annual rainfall datasets, even if largely employed in many areas in the world (see, among the others, de Asis and Omasa 2007; Wolka et al. 2015; Cartacuzencu et al. 2016; González-

Morales et al. 2018; Wang et al. 2018; Pal and Chakrabortty 2019) may not be adequate to predict the rainfall erosivity in Mediterranean areas (Capra et al. 2017).

It is also important to notice that the CUSUM test (Trend, 2012) applied to the R_i dataset in Fig. 6 shows a distinct change point in 2001 and this supports the hypothesis that the measurements of soil loss related to the study period 2006-2016 may not be representative of the long-term soil erosion in this area as they clearly overestimate soil loss (see Table 1). Again, this seems to confirm that the length of the observation record has an important impact on soil erosion estimates (Verstraeten et al. 2006) and suggests that care must be taken when a representative value of soil loss is requested for an area with lacks of data. Similar problems occur when calibration and/or validation exercises are necessary to establish the ability of a model to predict reliable values of soil erosion. For example, during the last 2-3 decades, alternative approaches, based on the use of fallout radionuclides (FRN), including mainly cesium-137 (^{137}Cs) and unsupported lead-210 ($^{210}Pb_{ex}$), proved to be very effective to assemble information on long-term and spatial patterns of erosion and deposition rates especially if coupled with existing traditional methods (Di Stefano et al. 2005; Porto and Walling 2015). These models need validation and the availability of a long-term representative value of soil erosion to be compared with the model estimate is a key issue. In this respect, Porto and Walling (2012) carried out a sampling campaign for ^{137}Cs and $^{210}Pb_{ex}$ analyses to estimate long-term soil erosion in the five plots used in this study. The overall results, updated to 2009, indicated that the estimates provided by ^{137}Cs, related to the period 1954-2006, were systematically lower that the measurements provided by the plots for the four-year period 2006-2009. The authors recognized that the four-year measurements of soil loss may have overestimated soil erosion and emphasized the need to consider a longer dataset to obtain a more reliable measured value. Also, a higher estimate of soil erosion obtained with the use of $^{210}Pb_{ex}$ suggested a possible increase of soil erosion rates during the previous 15-20 years. These results are well in agreement with our findings and suggest that the RUSLE model can be very effective for reconstructing long-term records of soil loss if reliable input datasets are available.

Another important indication can be inferred from Fig. 5 that shows the trend of soil loss reconstructed for plot 5. ~~A~~ The comparison with the ~~equivalent~~ estimates obtained from the other plots in Fig. 5 indicates that the amount of soil loss related to plot 5 is much lower. This result reflects the lower value of *Cm* calculated for this plot and suggests that the adoption of a proper strategy that includes the use of rotations with natural vegetation and conservative practices (mulching, no-tillage etc.) can be effective in reducing soil loss. This assumption is confirmed by several studies in the world that explored the effect of land use changes on soil loss (see, among the others, Maetens et al. 2012). In our case, the mean value of A_i for plot 5, related to the long-term period 1954-2019, is equal to 12.0 (t ha^{-1} yr^{-1}). This value is still a little higher than that (ca. 11.5 t ha^{-1} yr^{-1}) assumed by Bagarello et al. (2015) as tolerable soil loss for similar geographic contexts. However, it indicates that the adoption of the conservative practices described above allowed to reduce ~~it~~ soil loss significantly considering that the equivalent value obtained for plot 3 is ca. three times higher (31.9 t ha^{-1} yr^{-1}). This result is encouraging and suggests that an appropriate crop rotation is a key factor to minimize land degradation in these areas. In this respect, models like the RUSLE, based on empirical parameters of simple calculation, offer a good opportunity to predict soil loss for different scenarios and to evaluate possible countermeasures for long-term planning purposes.

5 CONCLUSIONS

The experimental plots used in this study provided important information on soil erosion rates obtained in an upland area of the Mediterranean environment. The first, important, result is related to the direct observations of soil loss obtained during the period of the experiment from 2006 to 2016. In this respect, the study demonstrated that direct measurements of soil loss can be misleading if the dataset cannot be extended for longer period. In order to avoid such problems, it is strongly suggested to account for long-term rainfall erosivity measurements in the absence of soil loss data. In the study area, the availability of rainfall data at short-time interval (5-30 minutes) from a local station allowed the calculation of the rainfall erosivity factor from 1954 to date. Based on this information, a RUSLE model was calibrated using the 11 years of soil loss measurements and it was applied to the extended period 1954-2019 to reconstruct the longer-term trend of soil erosion in the area. The overall results revealed that soil erosion has increased during this long-time window and showed a changing point at the beginning of the last two decades. These findings, in line with the results obtained from other authors, suggest that care must be taken when direct observations of soil loss are used for planning purpose as they could not be representative for the area under investigation for long-term periods. A second, important, result is related to the use of empirical models like RUSLE to predict soil loss for long periods. In this respect, the RUSLE model proved a good performance in its ability to reproduce soil loss rates in Mediterranean areas. However, the adoption of proper datasets of rainfall erosivity, derived from specific relationships between rainfall intensity and the *R*-factor, are strongly suggested and should be considered an essential tool to extend the representativeness of measurements.

Formatted: Font: Italic

Acknowledgements

This study has been finalized in the frame of Erasmus + KA2 - cooperation for innovation and the exchange of good practices - Capacity Building in the field of Higher Universities of Western Balkan Countries/SETOF. The authors are indebted to the ARPACAL for providing rainfall data used in this study. Thanks are also extended to both the anonymous referees and the Guest Editor for their useful comments.

Declarations

Consent to participate. All authors consented to participate in the study.

Consent for publication. All authors consented to the publication of the article.

Conflict of interest. The authors declare no competing interests.

References

Alexander LV (2016) Global observed long-term changes in temperature and precipitation extremes: A review of progress and limitations in IPCC assessments and beyond. Weather Clim Extremes 11:4-16

Arnoldus HMJ (1980) An approximation of the rainfall factor in the USLE. In: Assessment of Erosion. England: Wiley Chichester: 127–132

Bagarello V, Di Stefano C, Ferro V, Pampalone V (2010) Statistical distribution of soil loss and sediment yield at Sparacia experimental area, Sicily. Catena 82:45-52

Bagarello V, Di Stefano C, Ferro V, Pampalone V (2015) Establishing a soil loss threshold for limiting rilling. J Hydrol Eng 20(6):C5014001-1-C5014001-12

Bagarello V, Di Stefano C, Ferro V, Kinnel PIA, Pampalone V, Porto P, Todisco F (2011) Predicting soil loss on moderate slopes using an empirical model for sediment concentration. J Hydrol 400:267-273

Bagarello V, Ferro V, Pampalone V, Porto P, Todisco F, Vergni L (2018) Predicting soil loss in central and south Italy with a single USLE-MM model. J Soils Sediments 18(12):3365-3377

Bakker MM, Govers G, Kosmas C, Vanacker V, Van Oost K, Rounsevell M (2005) Soil erosion as a driver of land-use change. Agr Ecosyst Environ 105:467–481

Boardman J (2006) Soil erosion science: Reflections on the limitations of current approaches. Catena 68:73-86

Boardman J, Poesen J (2006) Soil Erosion in Europe. Wiley, Chichester. 878 pp

Brunetti M, Colacino M, Nanni T (2001) Trend in the daily intensity of precipitation in Italy from 1951 to 1996. Int J Climatol 21:299–316

Brunetti M, Maugeri M, Nanni T, Navarra A (2002) Droughts and extreme events in regional daily Italian precipitation series. Int J Climatol 22:1455–1471

Brunetti M, Buffoni L, Mangianti F, Maugeri M, Nanni T (2004) Temperature, precipitation and extreme events during the last century in Italy. Global Planet Change 40:141–149

Buffoni L, Maugeri M, Nanni T (1999) Precipitation in Italy from 1833 to 1996. Theor Appl Climatol 63:33–40

Capra A, Porto P, La Spada C (2017) Long-term variation of rainfall erosivity in Calabria (Southern Italy). Theor Appl Climatol 128(1-2):141-158

Cartacuzencu S, Coman A, Rosu G, Tincu R, Lazar G (2016) Analysis of hydric erosion produced by the Siret River, Romania during 1989-2008. Environ Eng Manag J 15:537-544

Cerdan O, Govers G, Le Bissonnais Y, Van Oost K, Poesen J, Saby N, Gobin A, Vacca A, Quinton J, Auerswald K, Klik A, Kwaad F J P M, Raclot D, Ionita I, Rejman J, Rousseva S, Muxart T, Roxo M J, Dostal T (2010) Rates and spatial variations of soil erosion in Europe: A study based on erosion plot data. Geomorphology 122:167–177

Chaplot V (2007) Water and soil resources response to rising levels of atmospheric CO_2 concentration and to changes in precipitation and air temperature. J Hydrol 337:159-171

Cinnirella S, Iovino F, Porto P, Ferro V (1998) Anti-erosive effectiveness of Eucalyptus coppices through the cover management factor estimate. Hydrol Process 12(4):635-649

De Araújo JC, Güntner A, Bronstert A (2006) Loss of reservoir volume by sediment deposition and its impact on water availability in semiarid Brazil. Hydrolog Sci J 51(1):157-170

de Asis A M, Omasa K (2007) Estimation of vegetation parameter for modeling soil erosion using linear Spectral Mixture Analysis of Landsat ETM data. ISPRS J Photogramm Remote Sens 62:309-324

Di Stefano C, Ferro V, Porto P. (1999) Linking sediment yield and caesium-137 spatial distribution at basin scale. J Agric Eng Res 74:41–62

Di Stefano C, Ferro V, Porto P, Rizzo S (2005) Testing a spatially distributed sediment delivery model (SEDD) in a forested basin by caesium-137 technique. J Soil Water Conserv 60(3):148–157

~~Du D, Zhao X, Huang R (2017) The impact of climate change on developed economies. Econ Lett 153:43-46~~

Evans R (1995) Some methods of directly assessing water erosion of cultivated land – a comparison of measurements made on plots and in fields. Prog Phys Geog 19(1):115–129

Favis-Mortlock D, Boardman J (1995) Nonlinear responses of soil erosion to climate change: A modeling study on the UK South Downs. Catena 25:365-387

Ficklin D L, Luo Y, Luedeling E, Zhang M (2009) Climate change sensitivity assessment of a highly agricultural watershed using SWAT. J Hydrol 374(1):16–29

Foster GR, McCool DK, Renard KG, Moldenhauer WC (1981) Conversion of the universal soil loss equation to SI metric units. J Soil Water Conserv 36(6):355-359

Fournier F (1960) Climat et erosion. Presses Universitaries de France, Paris

González-Morales SB, Mayer A, Ramírez-Marcial N (2018) Assessment of soil erosion vulnerability in the heavily populated and ecologically fragile communities in Motozintla de Mendoza, Chiapas, Mexico. Solid Earth 9:745-757

Hirsch RM, Helsel DR, Cohn TA, Gilroy EJ (1992) Statistical analysis of hydrologic data. In: Maidment DR (ed) Handbook of Hydrology, McGraw-Hill, pp. 1711-1730

IPCC (2018) Special Report on Global Warming of 1.5°C, https://www.ipcc.ch/reports/ October 2018

Karl TR, Knight RW (1998) Secular Trends of Precipitation Amount, Frequency, and Intensity in the United States. Bull Am Meteorol Soc 79:231-241

Khodadadi M, Zaman M, Mabit L, Blake WH, Gorji M, Bahrami AS, Meftahi M, Porto P (2020) Exploring the potential of using ^{7}Be measurements to estimate soil redistribution rates in semi-arid areas: results from Western Iran and Southern Italy. J Soils Sediments 20(9):3524-3536

Loughran RJ (1989) The measurement of soil erosion. Prog Phys Geogr 13:216-233

Maetens W, Poesen J, Vanmaercke M (2012) How effective are soil conservation techniques in reducing plot runoff and soil loss in Europe and the Mediterranean? Earth-Sci Rev 115:21–36

Mason SJ, Waylen PR, Mimmack GM, Rajaratnam B, Harrison JM (1999) Changes in extreme rainfall events in South Africa. Clim Change 41:249–257

McCool DK, Brown LC, Foster GR, Mutchler CK, Meyer LD (1987) Revised slope steepness factor for the universal soil loss equation. Trans ASAE 30(5):1387-1396

McCool DK, Foster GR, Mutchler CK, Meyer LD (1989) Revised slope length factor for the Universal Soil Loss Equation. Trans ASAE 32(5):1571-1576

~~Miyan MA (2015) Droughts in Asian Least Developed Countries: Vulnerability and sustainability. Weather Clim Extremes 7:8-23~~

Moberg A, Jones PD (2005) Trends in indices for extremes in daily temperature and precipitation in central and western Europe. Int J Climatol 25:1149– 1171

Nearing MA, Foster GR, Lane LJ, Finkner SC (1989) A process-based soil erosion model for USDA- water erosion prediction project technology. Trans ASAE 32:1587–1593

Osborn TJ, Hulme M, Jones PD, Basnett TA (2000) Observed trends in the daily intensity of United Kingdom precipitation. Int J Climatol 20:347–364

Pal SC, Chakrabortty R (2019) Simulating the impact of climate change on soil erosion in sub-tropical monsoon dominated watershed based on RUSLE, SCS runoff and MIROC5 climatic model. Adv Space Res 64:352–377

Palmer MA, Lettenmaier DP, Poff NL, Postel SL, Richter B, Warner R (2009) Climate Change and River Ecosystems: Protection and Adaptation Options. Environ Manage 44:1053–1068

Pandey BK, Gosain AK, Paul G, Khare D (2017) Climate change impact assessment on hydrology of a small watershed using semi-distributed model. Appl Water Sci 7:2029–2041

Field Code Changed

Pimentel D, Harvey C, Resosudarmo P, Sinclair K, Kurz D, McNair M, Crist S, Shpritz L, Fitton L, Saffouri L, Blair R (1995) Environmental costs of soil erosion and conservation benefits. Science 267:1117–1123

Porto P (2016) Exploring the effect of different time resolutions to calculate the rainfall erosivity factor R in Calabria, southern Italy. Hydrol Process 30:1551-1562

Porto P, Callegari G (2021) Using ^{7}Be measurements to explore the performance of the SEDD model to predict sediment yield at event scale. Catena 196: 104904

Porto P, Walling DE (2012) Validating the use of ^{137}Cs and $^{210}Pb_{ex}$ measurements to estimate rates of soil loss from cultivated land in southern Italy. J Environ Radioact 106:47-57

Porto P, Walling DE (2015) Use of caesium-137 Measurements and long-term records of sediment load to calibrate the sediment delivery component of the SEDD model and explore scale effect: examples from Southern Italy. J Hydrol Eng 20(6)

Porto P, Walling DE, La Spada C, Callegari G (2016) Validating the use of ^{137}Cs measurements to derive the slope component of the sediment budget of a small catchment in southern Italy. Land Degrad Dev 27:798–810

Porto P, Walling DE, Callegari G (2018) Using repeated ^{137}Cs and $^{210}Pb_{ex}$ measurements to establish sediment budgets for different time windows and explore the effect of connectivity on soil erosion rates in a small experimental catchment in Southern Italy. Land Degrad Dev 29:1819-1832

Preiti G, Romeo M, Bacchi M, Monti M (2017) Soil loss measure from Mediterranean arable cropping systems: Effects of rotation and tillage system on C-factor. Soil Till Res 170:85–93

Pruski FF, Nearing MA (2002a) Runoff and soil loss changes expected for changes in precipitation patterns under global climate change. J Soil Water Conserv 57:7-16

Pruski FF, Nearing MA (2002b) Climate-induced changes in erosion during the 21st century for eight U.S. locations. Water Resour Res 38(12):1298, doi:10.1029/2001WR000493

Renard KG, Foster GR, Yoder DC, McCool DK (1994) RUSLE revisited: status, questions, answers, and the future. J Soil Water Conserv 49:213-220

Renard KG, Foster GR, Weesies GA, McCool DK, Yoder DC (1997) Predicting Soil Erosion by Water: A Guide to Conservation Planning with the Revised Universal Soil Loss Equation (RUSLE), Agric. Handbk., vol. 703, U. S. Dep. of Agric., Washington, D. C.

Romero-Díaz A, Ruiz-Sinoga JD, Robledano-Aymerich F, Brevik EC, Cerdà A (2017) Ecosystem responses to land abandonment in Western Mediterranean Mountains. Catena 149:824-835

Shao Z, Sumari NS, Portnov A, Ujoh F, Musakwa W, Mandela PJ (2021) Urban sprawl and its impact on sustainable urban development: a combination of remote sensing and social media data. Geo Spat Inf Sci 24(2):241-255

~~Shiferaw B, Tesfaye K, Kassie M, Abate T, Prasanna BM, Menkir A (2014) Managing vulnerability to drought and enhancing livelihood resilience in sub-Saharan Africa: Technological, institutional and policy options. Weather Clim Extremes 3:67-79~~

Suppiah R, Hennessy KJ (1998) Trends in total rainfall, heavy rain events and numbers of dry days in Australia, 1910–1990. Int J Climatol 18:1141–1164

Verstraeten G, Poesen J, Demaree G, Salles C (2006) Long-term (105 years) variability in rain erosivity as derived from 10- min rainfall depth data for Ukkel (Brussels, Belgium): implications for assessing soil erosion rates. J Geophys Res 111:D22

Wang M, Baartman JE, Zhang H, Yang Q, Li S, Yang J, Cai C, Wang M, Ritsema CJ, Geissen V (2018) An integrated method for calculating DEM-based RUSLE LS. Earth Sci Inform 11:579–590

Wen Y, Schoups G, van de Giesen N (2017) Organic pollution of rivers: Combined threats of urbanization, livestock farming and global climate change. Nature Sci Rep 7:43289

Wischmeier WH, Johnson CB, Cross BV (1971) A soil erodibility nomograph for farmland and construction sites. J Soil Water Conserv 26:189-193

Wischmeier WH, Mannering JV (1969) Relation of soil properties to its erodibility. Soil Sci Soc Am Proc 39:131-137

Wischmeier WH, Smith DD (1978) Predicting Rainfall-erosion Losses. A Guide to Conservation Farming, vol. 537. US Dept. of Agric., Agr. Handbook, pp. 151

Wolka K, Tadesse H, Garedew E, Yimer F (2015) Soil erosion risk assessment in the Chaleleka wetland watershed, Central Rift Valley of Ethiopia. Environ Syst Res 4:1-12

Yi Y, Wang Z, Zhang K, Yu G, Duan X (2008) Sediment pollution and its effect on fish through food chain in the Yangtze River. Int J Sediment Res 23(4):338-347

Table 1

	R (MJ mm ha^{-1} h^{-1} yr^{-1})	**K** (t ha h ha^{-1} MJ^{-1} mm^{-1})	**Cm**	**LS**	**A_i (2006-2016)** (t ha^{-1} yr^{-1})	**A_i (1954-2019)** (t ha^{-1} yr^{-1})
Plot 1	5032	0.011	1.00	1.20	69.5	56.1
Plot 2			0.38	1.27	28.6	22.5
Plot 3			0.50	1.36	39.2	31.9
Plot 4			0.41	1.35	32.2	25.7
Plot 5			0.21	1.25	14.4	12.0

Figure Captions

Fig. 1 The study area and the experimental plots

Fig. 2 Values of soil loss obtained from each plot for the study period 2006-2016. The graph in (a) shows the frequency distribution of the annual values. The box plot in (b) indicates the data distribution

Fig. 3 Calculation of the soil erodibility factor *K*

Fig. 4 The frequency distribution of C_i for each plot. The dashed line represents a log-normal theoretical distribution

Fig. 5 The annual soil loss reconstructed for each plot for the period 1954-2019. Grey bars indicate the estimated values while white bars report the measured values obtained for the study period

Fig. 6 The annual values (R_i) of the rainfall erosivity factor obtained for the period 1954-2019 (a) and the annual values of rainfall measured in the same period (b)

Figure 1

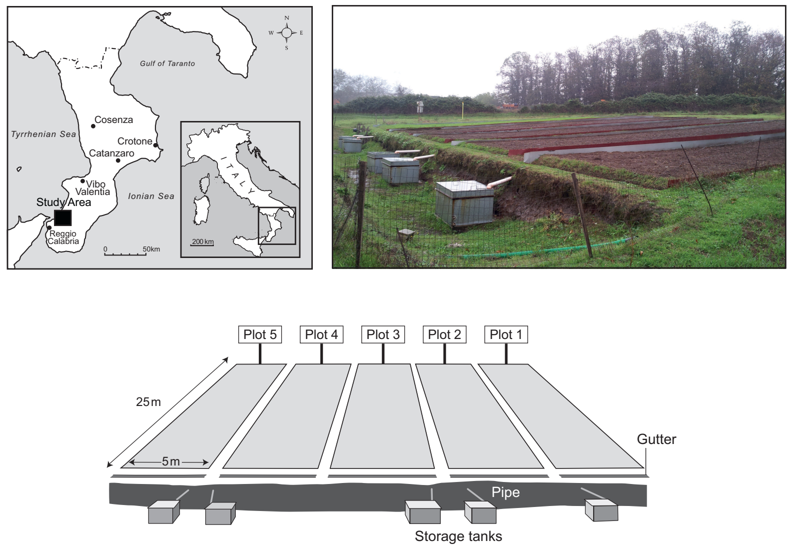
N
W
E
S
Gulf of Taranto
Cosenza
Tyrrhenian Sea
Crotone
Catanzaro
Vibo Valentia
Ionian Sea
Study Area
Reggio Calabria
0
50km
ITALY
200 km
Plot 5
Plot 4
Plot 3
Plot 2
Plot 1
25m
5m
Gutter
Pipe
Storage tanks

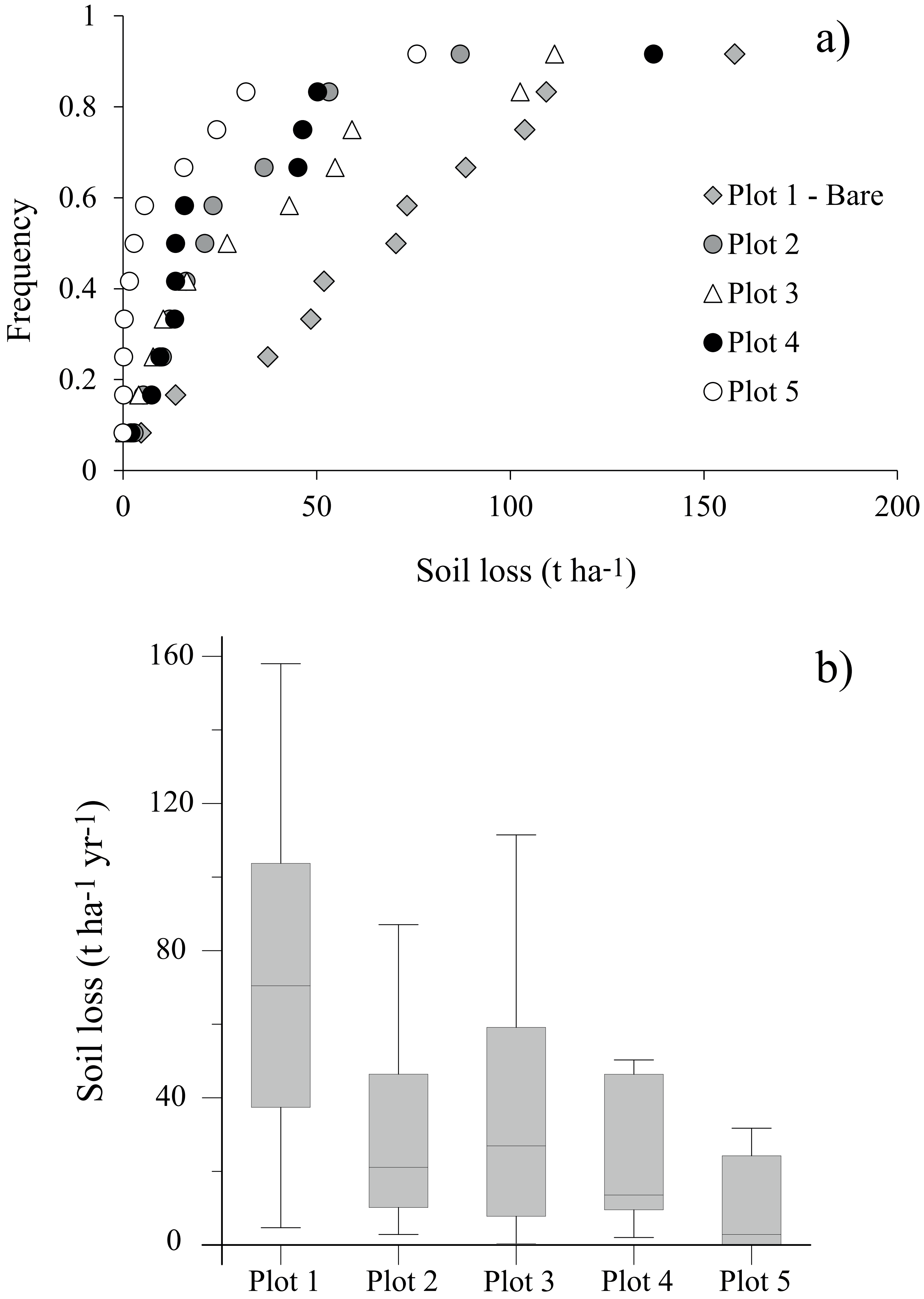
a)
Frequency
0
0.2
0.4
0.6
0.8
1
0
50
100
150
200
Soil loss (t ha-1)
Plot 1 - Bare
Plot 2
Plot 3
Plot 4
Plot 5
b)
Soil loss (t ha-1 yr-1)
0
40
80
120
160
Plot 1
Plot 2
Plot 3
Plot 4
Plot 5

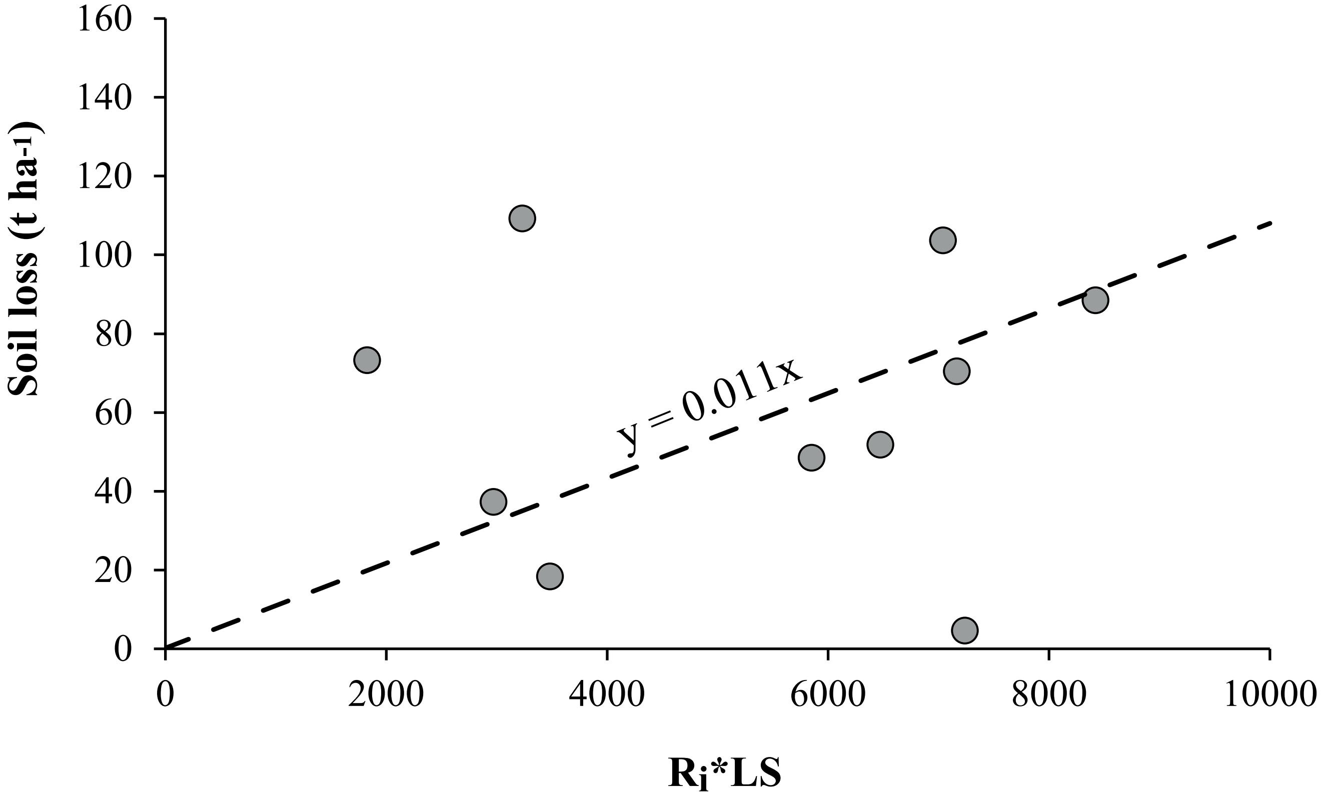
Soil loss (t ha-1)
0
20
40
60
80
100
120
140
160
0
2000
4000
6000
8000
10000
y = 0.011x
Ri*LS

Figure 4

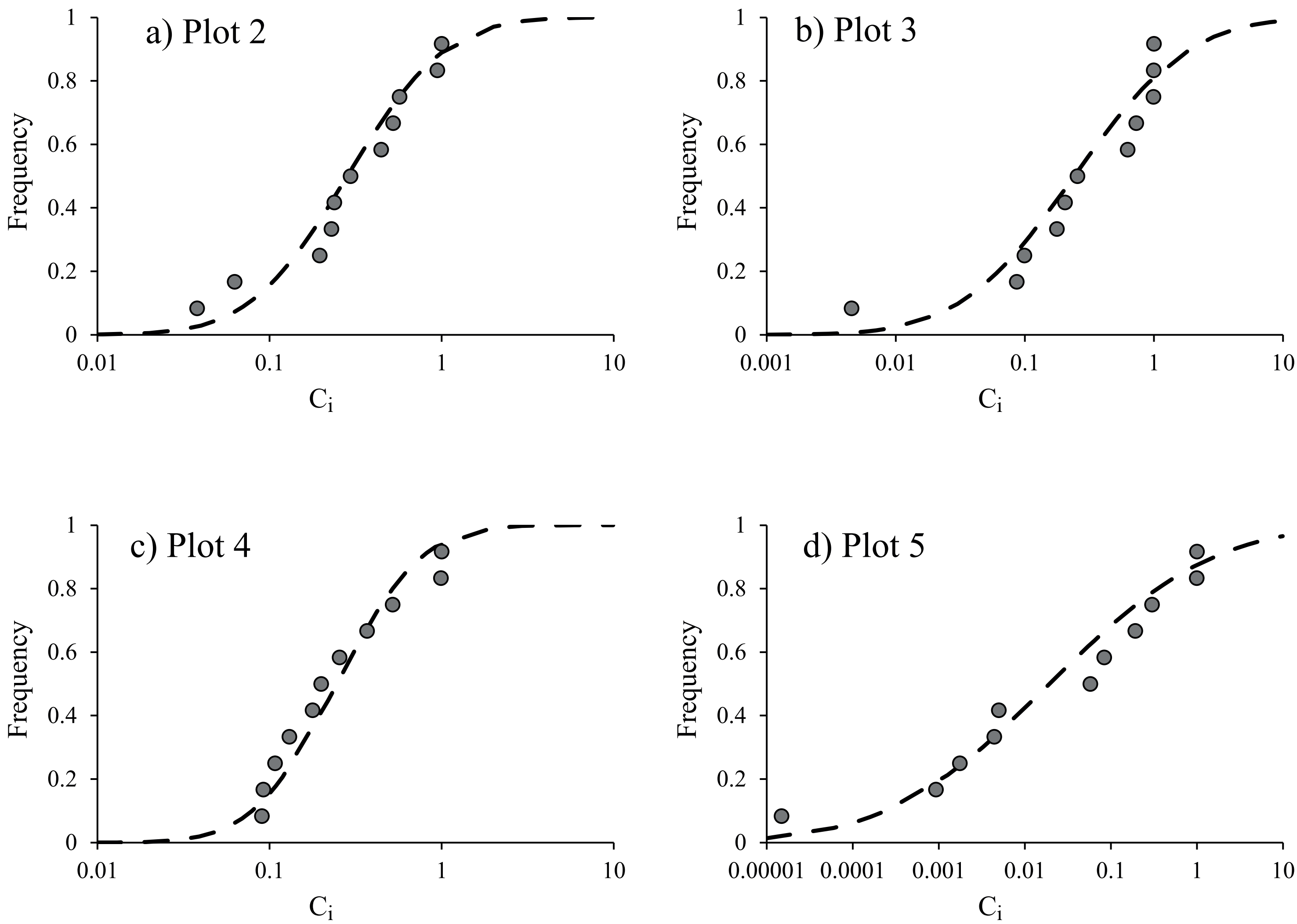
a) Plot 2
b) Plot 3
c) Plot 4
d) Plot 5
Frequency
0
0.2
0.4
0.6
0.8
1
0.01
0.1
1
10
0.001
0.00001
0.0001
Ci

Figure 5

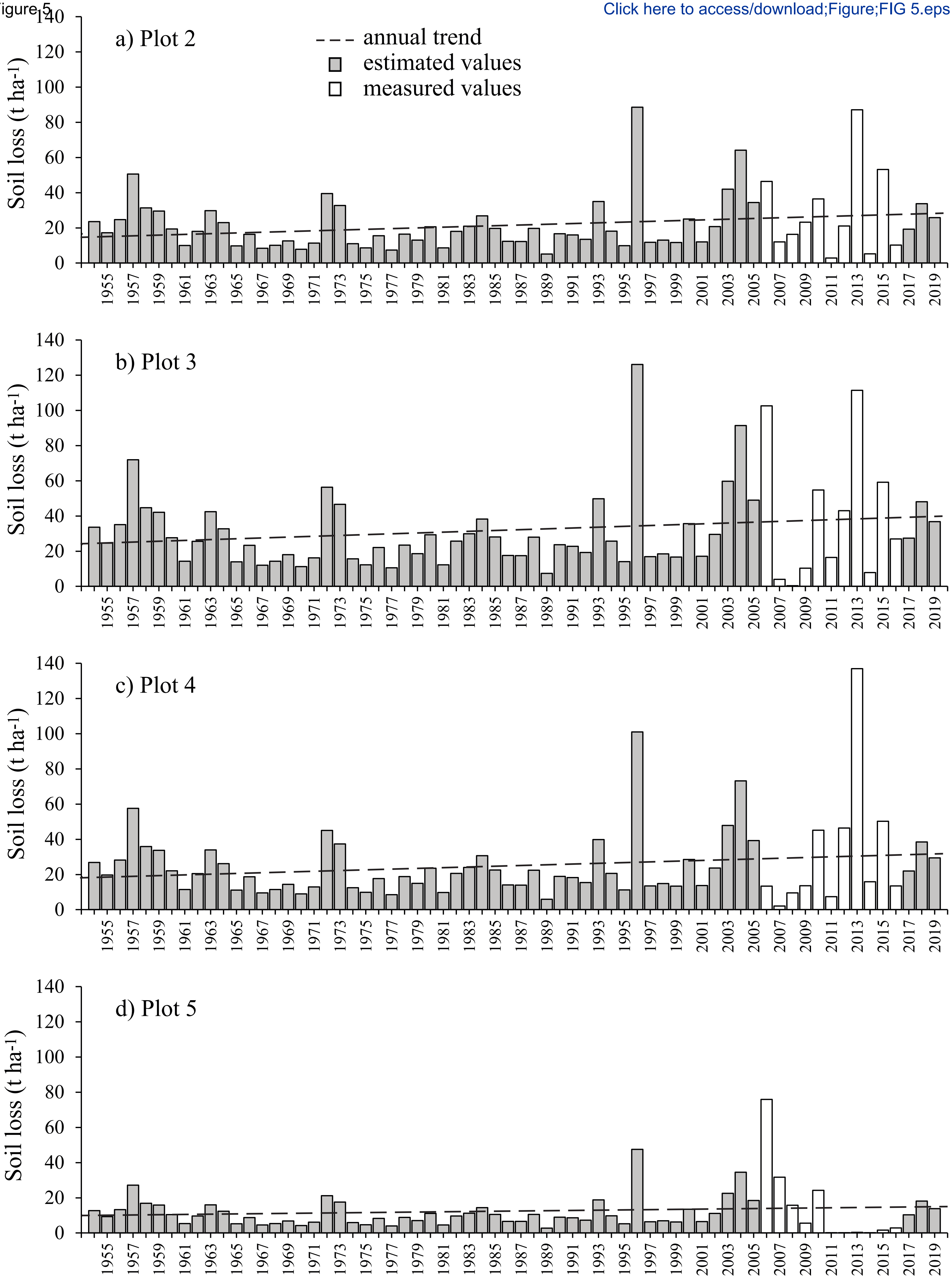
a) Plot 2
annual trend
estimated values
measured values
b) Plot 3
c) Plot 4
d) Plot 5
Soil loss (t ha-1)
0
20
40
60
80
100
120
140
1955
1957
1959
1961
1963
1965
1967
1969
1971
1973
1975
1977
1979
1981
1983
1985
1987
1989
1991
1993
1995
1997
1999
2001
2003
2005
2007
2009
2011
2013
2015
2017
2019

Figure 6 Click here to access/download;Figure;FIG 6ab.pdf